NUCLEAR SCIENCE AND TECHNIQUES **26**, 010202 (2015)

Instrumentation and application of the ion beam analysis line of the in situ ion beam system*

HUANG Zhi-Hong (黄志宏),[1] ZHANG Zao-Di (张早娣),[1]
WANG Ze-Song (王泽松),[1] WANG Lang-Ping (王浪平),[2] and FU De-Jun (付德君)[1,†]

[1]*Accelerator Laboratory, Key Laboratory of Artificial Micro- and Nano-Materials of Ministry of Education of China, School of Physics and Technology, Wuhan University, Wuhan 430072, China*
[2]*State Key Laboratory of Advanced Welding and Joining, Harbin Institute of Technology, Harbin 150001, China*

(Received March 12, 2014; accepted in revised form April 9, 2014; published online February 2, 2015)

An ion beam analysis system was established on a 1.7 MV tandem accelerator, enabling Rutherford backscattering (RBS), elastic recoil detection (ERD), nuclear reaction analysis (NRA) and channeling measurements. The system was tested by performing qualitative and quantitative analysis of Si, Ni/Si, $BiFeO_3$:La/Si, MoC/Mo/Si and TiBN/Si samples. RBS of a $BiFeO_3$:La film was used as system calibration. Tested by ion beam channeling, a Si(100) is of good crystallinity (χ_{min} = 3.01%). For thin film samples, the measured thickness agrees well with simulation results by SIMNRA. In particular, composition of a MoC/Mo/Si and TiBN film samples were analyzed by RBS and non-Rutherford elastic backscattering.

Keywords: Ion beam analysis, Channeling, Rutherford backscattering, Non-Rutherford elastic backscattering

DOI: 10.13538/j.1001-8042/nst.26.010202

I. INTRODUCTION

Based on interactions of energetic ions with target materials, ion beam analysis techniques are widely used in characterization of thin films and multilayer structures. They provide quantitative information of elemental components of the solid from several atomic layers to micrometer depth from the surface, or depth profiling of impurities. Therefore, it attracted much attention in the ion beam community and many ion beam systems have been developed and upgraded. These include conventional ion beam analysis, microbeams [1–4], and combination of ion beam systems, such as the 5 MV tandem accelerator interfaced with the 200 MeV proton synchrotron in the Wakasa Wan Energy Research Center [5] and the multi-ion irradiation platform JANNUS (Joint Accelerators for Nano Sciences and Nuclear Simulation) at Saclay where the first triple beam irradiation using Fe, He and H ion beams was carried out in 2010 [6].

Ion beam analysis methods are frequently used due to their efficiency in providing a broad spectrum of qualitative and quantitative information on elemental composition and crystal structure of solids. While Rutherford backscattering (RBS) provides composition and depth profiles of heavy elements in a light matrix, elastic recoil detection analysis (ERDA) is unique in profiling light elements (C, B, Li, H etc.) in a heavy matrix. Nuclear reaction analysis (NRA) provides specific elemental profiling which can resolve isotopes. Proton induced X-ray emission (PIXE) enables simultaneous detection of elements of intermediate atomic numbers. Ion beam channeling, compared with random ion beam scattering spectroscopy, gives high precision measurement of crystallinity of single-crystalline wafers or epitaxial layers [7]. Ion beam analysis methods have a common advantage of non-destructiveness in the sense that the corresponding ion-solid interactions do not consume the target material, since the beam current is at analytical level, i.e., a few *n*A. Damage may result only, for sensitive samples, from ionization or heating by the ion beams, sputtering or nuclear stopping and in the case of channeling studies in single crystals, from defect production inducing dechanneling [8].

The accelerator system in Wuhan University is multifunction equipment, namely, the 1.7 MV tandem accelerator is interfaced with a 200 kV ion implanter and a transmission electron microscope (TEM). The ability of ion beam technique is extended to emerging fields of physics and materials science. In the present work, we have designed RBS/PIXE/C system aiming at characterization of solids with a broad range of elements in the same chamber and *in situ* measurement of the implanted sample in a dual beam chamber. The advantage of low-energy RBS technique lies in its capability of quantitative analysis of major and minor constituents lying in the first 0.5–2.0 μm of a material depending on the sample structure and composition. And the detection limits for some light elements may further be improved by using resonant scattering. In this paper we report the tests of basic functions of the system based on RBS and channeling, and demonstrate quantitative characterization of elemental profiling, and interface analysis, and crystal quality of wafers and thin film materials.

II. SYSTEM DESIGN

Figure 1 shows a schematic diagram of the *in situ* ion beam system. Ion beams extracted from the negative ion source by cesium sputtering (SNICS) are transported to the low energy cluster ion beam chamber for low energy ion implantation or to the RBS/PIXE/C chamber after transportation lines of the tandem accelerator. The dual beam chamber is used for

* Supported by the National Natural Science Foundation of China (No. 11405117) and the State Key Lab of Advanced Welding and Joining of Harbin Institute of Technology (No. AWJ-M13-03)
† Corresponding author, djfu@whu.edu.cn

in situ implantation with ions from the tandetron or 200 kV implanter. It will also be possible to conduct *in situ* ion beam analysis of the implanted samples with the establishment of the RBS/PIXE/C system in the dual beam chamber. The ion beam analysis line thus consists of the SNICS, tandetron and analysis chamber.

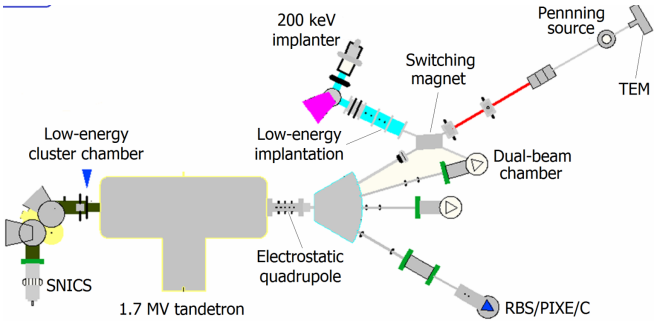

Fig. 1. (Color online) Schematic diagram of the *in situ* ion beam system.

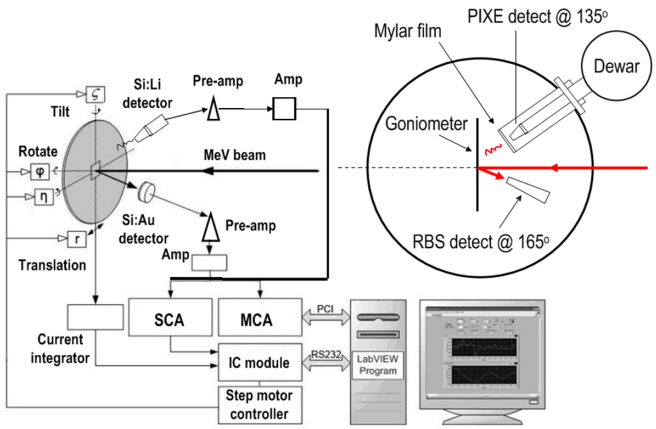

Fig. 2. (Color online) Schematic diagram of the measurement system of the ion beam analysis line.

A schematic diagram of the measurement system is shown in Fig. 2. Conventional ion beam scattering, recoil detection and nuclear reaction are performed with Si:Au surface barrier detectors (SBD) connected through a charge sensitive preamplifier, an amplifier and a multichannel analyzer (MCA). The total number of ions is recorded by a charge integrator. For channeling measurement, a single channel analyzer (SCA) and a linear rate-meter are used. For PIXE measurement, we have an Ortec SLP-1080 detector with liquid nitrogen cooling and a miniature detector XR-100CR with thermal electric cooling. The SLP-1080 detector is put into the chamber through a cinlyndrical port. The XR-100CR detector is placed in the chamber, and the electronics for the RBS measurement can be used for signal amplification and recording.

Ion beams extracted from the SNICS are focused and deflected before they were accelerated to 1–3 MeV, depending on energy requirement for different measurements. The accelerated ion beams are focused again by the electrostatic quadrupole lens and deflected into the analysis chamber by a magnetic switcher. The samples are placed on a ϕ70 mm copper holder mounted on a four-axis goniometer, which is computer controlled through a stepping motor controller. During the measurement, the stepping motor controller controls movement of the goniometer, providing three orthogonal rotations (two tilts and one azimuth) and one translation (y-axis). The z-axis is aligned with the incident ion beam direction. The y-axis is defined by orthogonality with both the x- and z-axis, which complete a right-hand triad. Specification of the sample orientation is described by three angles, γ, η and ζ, corresponding to rotation of the x-, y- and z-axes, respectively. The goniometer enables the samples to move along the y-axis or rotate around the x-, y- and z-axes. The spatial relationship between the sample and incident ion beam is described by the angle $\theta = (\eta^2 + \zeta^2)^{1/2}$ and the azimuthal angle φ.

In RBS analysis, the ion beam was collimated to 0.3 mm size by an aperture slot. The SBD, with an effective area of 50 mm^2, is positioned at a distance of 10–15 cm to the sample and 150°–170° to the beam incidence. The signals, after preamplifier and the spectroscopic amplifier, were sent to the MCA installed in the computer. The current integrator records the charge collected during the experiment.

The RBS/C measurement has three more steps. First, signals from the amplifier are sent to a gate interface of the MCA through a single channel analyzer (SCA), simultaneously, an energy window is selected through coincidence by regulating the upper and lower level discriminators of the SCA. Next, the gate interface is disconnected and signals of the selected energy range from the SCA are sent to the linear rate-meters. Finally, tilt or rotation of the crystal sample relative to the beam incidence is controlled by the stepping motor controller, and the reduction of scattering yield is displayed on the linear rate-meters to decide channeling effect of the incident beams [9]. Detailed information of how to determine the channel of crystal sample by computerized control program was described in the literature [10].

III. ANALYSIS AND DISCUSSION

A. System calibration and determination of crystal quality

The RBS system was calibrated by measuring the Au peak position and Si edge of a Au-deposited Si sample. RBS measurement of a $BiFeO_3$:La layer sample was performed. $BiFeO_3$ is a typical multiferroic material with ferroelectric and antiferromagnetic properties, has and is of broad application prospects in spintronics and multibit memory devices. Doping it with rare earth elements may significantly improve its ferroelectric and ferromagnetic properties. It is important to measure each element accurately. A thin film of La-doped $BiFeO_3$ was prepared by sol gel method on a Si(100) substrate. Fig. 3(a) shows RBS spectrum of the sample using 2.9 MeV $^7Li^{2+}$ beams with a backscattering angle of 160°. The leading edge of Si is at channel 147 (at half-height) and the Bi, La, Fe and O peak positions are at channel numbers of

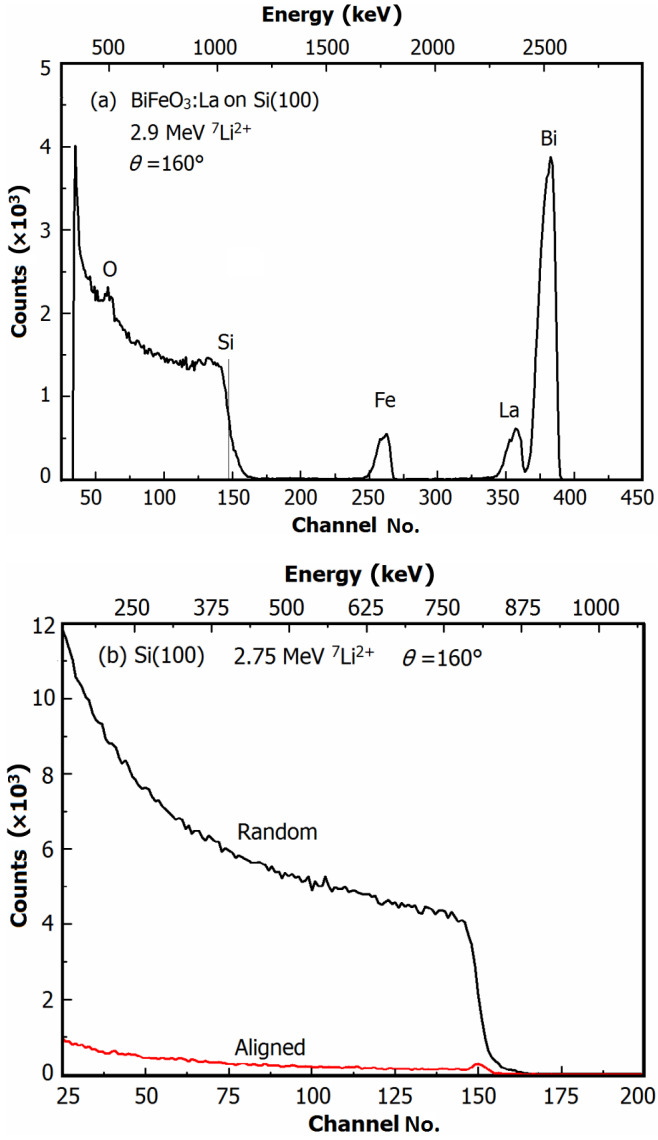

Fig. 3. (Color online) RBS spectrum of La-doped $BiFeO_3$ film on Si (100) (a) and RBS/C spectrum of single-crystal Si (100) (b).

386, 362, 265, and 62, respectively. They correspond to the kinematic factors of 0.8778 for Bi, 0.8219 for La, 0.6126 for Fe, 0.3713 for Si, and 0.1607 for O. This indicates that Li ion beam has excellent mass resolution for many elements of film analysis. Assuming that the deposited La-$BiFeO_3$ thin layer is distributed uniformly on the substrate, the film thickness is estimated at 135 nm. Compared with other methods, the RBS analysis is very accurate, with an error of just 2%.

Figure 3(b) shows RBS/C measurement results of a single crystal Si(100) sample using 2.75 MeV Li ion beams. Compare to the random spectrum, the backscattering yield greatly reduced in the aligned spectrum, the flat shape of which demonstrates that the incident ions go deeply into the crystal channels without dechanneling. At the high-energy edge, a small peak was observed, revealing an amorphous layer in the surface owning to the cutting during sample preparation. The minimum yield, χ_{min}, defined as the backscattered yield ratio of the aligned spectrum to the random spectrum in the same channel region, i.e., the same depth, represents structural quality of the whole lattice of a monatomic crystal. For a perfect crystal, χ_{min} could be 1–2% [9]. The measured χ_{min} for the Si(100) sample is 3.01%, indicating a high quality crystal structure.

B. Quantitative analysis of thin films

Thickness of a Ni film prepared by electron beam evaporation on SiO_2:Si substrate was measured by RBS with 2.9 MeV $^7Li^{2+}$ in normal incidence at a backscattering angle of 160° (Fig. 4). The yield of backscattered Li ions was detected by a Si:Au surface barrier detector with an effective detection area of 50 mm^2, positioned at 112.6 mm from the sample, with a solid angle of Ω = 3.94 msr. The measured spectrum overlaps with the theoretical spectrum simulated using the iterative analytical code of SIMNRA. The simulated areal density of the Ni film is 2.21×10^{18} atoms/cm^2, corresponding to a thickness of 242 nm. From the measured spectrum, the Ni peak area is A = 510 000 cts, and the areal density $Nt = 2.20 \times 10^{18}$ atoms/cm^2, corresponding to a thickness of 240 nm, using the equation of $Nt = A/\sigma\Omega Q$, where the scattering cross section of Ni being σ = 1.25 bar from $d\sigma/d\Omega = [Z_1 Z_2 e^2/(4E)]2(4/\sin^2\theta)$, and the number of incident ions being $Q = 4.7 \times 10^{13}$(7.5 μC).

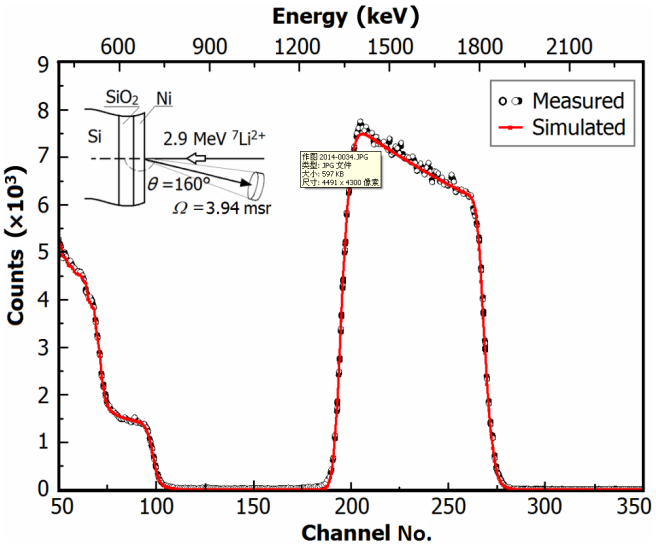

Fig. 4. (Color online) RBS spectrum of a Ni film on SiO_2/Si substrate, and the simulated spectrum using SIMNRA.

C. Composition analysis of multi-element and multilayer samples

A MoC thin film was prepared by multi-arc ion plating on Si substrate with Mo film as a transition layer. The Mo

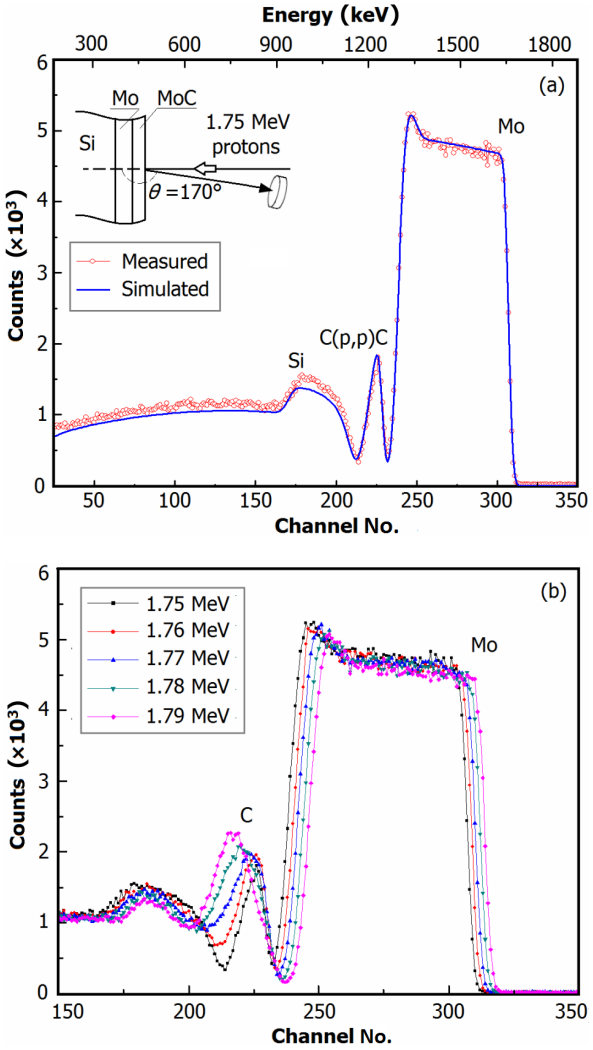

Fig. 5. (Color online) The measured and simulated RBS-spectra (a) for 1.75 MeV protons backscattered from MoC film deposited on Si substrates with Mo as a transition layer, and RBS spectra of MoC/Mo/Si at 1.75–1.79 MeV(b).

and C contents, and thickness of the MoC film, were determined by RBS analysis using a 1.75 MeV proton beam and the backscattering angle of $\theta = 170°$. The RBS spectra are shown in Fig. 5(a) together with a fit using the SIMNRA code. The Mo signal is approximately a rectangular peak with the front edge rising sharply. It indicates that molybdenum in the MoC layer is quite uniformly distributed and the hump at the back edge is the signal of Mo from transition layer. The carbon signal is a sharp peak rather than a hillock. Because non-Rutherford elastic backscattering occurred for carbon and the non-Rutherford backscattering cross section is 60 times larger than that of Rutherford backscattering at 1.74 MeV. [7] With 1.75 MeV protons, non-Rutherford elastic backscattering of carbon occurred at depth near the surface. A raised Si edge can also be observed due to the enhanced elastic scattering cross-section for Si atoms at 1.75 MeV of protons. According to the simulation result, the content of Mo is 0.71 and the

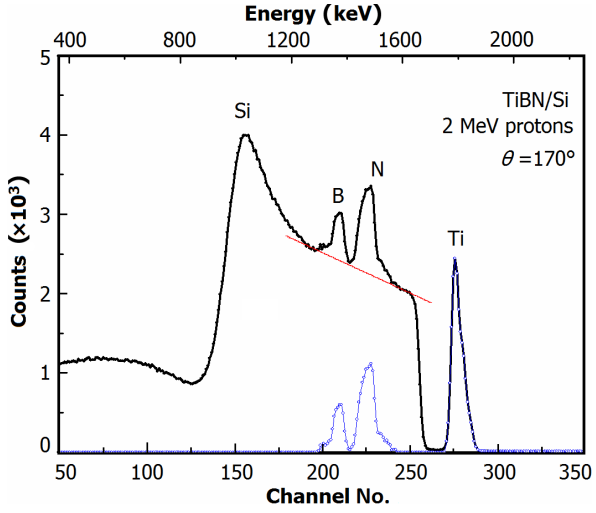

Fig. 6. (Color online) Light elements analysis of TiBN film by non-Rutherford resonance scattering.

content of C is 0.29 in the compound film layer with an area density of 1.52×10^{19} atom/cm^2. The Mo transition layer is 296.4 nm in thickness. Fig. 5(b) shows RBS spectra of the sample measured under energies of 1.75–1.79 MeV. It can be seen that the spectrum broadened and the C peaks moved to the low energy region with increasing incident beam energy, due to that occurrence of non-Rutherford elastic backscattering of carbon deepened with the proton energy, and the energy resolution worsened with increasing proton energy.

D. The detection and analysis of light elements in compound film

It is quite difficult to detect films containing light elements on a substrate of higher atomic mass by backscattering techniques, in which the yield of substrate is too high to distinguish signals of the light elements. In this case, one can use resonant scattering, which is of greater scattering cross section than Rutherford scattering. Appropriate higher energy should be applied so that resonance nuclear reaction occurs for certain elements.

A sample of TiBN film deposited on Si substrate by multi-arc ion plating method was analyzed by 2 MeV proton with a backscattering angle of $\theta = 170°$. Fig. 6 is the energy spectra of the sample, with the fitting line and spectrum of the TiBN film after subtraction of Si substrate. The strong non-Rutherford resonances in ^{1}H–^{14}N and ^{1}H–^{11}B cross sections lead to sufficient enhancement of the N and B signals and areal density of the film can be calculated with the peak areas. The net integrated counts of the Ti, N and B peaks in the blue spectrum are $A_{Ti} = 186\,921$ cts, $A_N = 118\,432$ cts and $A_B = 47\,248$ cts, respectively. A large uncertainty may be caused by subtraction of the substantial signal due to the Si substrate. Accuracy of the N and B yields is determined by the error of intercept and slope of the straight regression line $y = y_0 + kx$, where y is an approximation of the yield Y in

channel x, y_0 is the intercept and k is the slope, best fitted into the experimental data. With 2 MeV protons, the cross section of Ti is Rutherford and the cross sections of N and B are non-Rutherford. The ^{1}H−^{14}N cross-section enhancement factor is $(\sigma/\sigma_R)_N = 5$ and the ^{1}H−^{11}B factor is $(\sigma/\sigma_B)_N = 7$ [7]. The cross section of Rutherford backscattering of Ti, B and N can be calculated as

$$\sigma_{R,Ti}(E_0, 170^\circ) = (0.6359/2^2) \times 10^{-24} = 1.590 \times 10^{-25}\ \mathrm{cm^2/sr}, \quad (1)$$

$$\sigma_{R,N}(E_0, 170^\circ) = (0.0638/2^2) \times 10^{-24} = 1.595 \times 10^{-26}\ \mathrm{cm^2/sr}, \quad (2)$$

$$\sigma_{R,B}(E_0, 170^\circ) = (0.0323/2^2) \times 10^{-24} = 8.078 \times 10^{-27}\ \mathrm{cm^2/sr}. \quad (3)$$

The number of backscattered particles detected using the surface energy approximation for normal incidence of beam can be expressed as $A_0 = \sigma(E_0)\Omega Q N t$, where $\sigma(E_0)$ is scattering cross-section at incident proton energy E_0, Ω is solid angle, Q is incident proton flux, N is number density of target atoms, and t is film thickness. Then, for Ti: N and Ti: B ratios from the backscattered spectrum, we have

$$N_{Ti}/N_N = (A_{Ti}/A_N)[\sigma_{R,N}(E_0, 170^\circ)/\sigma_{R,Ti}(E_0, 170^\circ)](\sigma/\sigma_R)_N, \quad (4)$$

$$N_{Ti}/N_B = (A_{Ti}/A_B)[\sigma_{R,B}(E_0, 170^\circ)/\sigma_{R,Ti}(E_0, 170^\circ)](\sigma/\sigma_R)_B. \quad (5)$$

The average stoichiometric ratio for this film was calculated as Ti:N:B=1.4:1.75:1.

IV. CONCLUSION

Measurements were carried out by ion beam analysis establishment on the 1.7 MV tandem accelerator at Wuhan University. The RBS spectrum calibration using a $BiFeO_3$:La/Si sample indicates that the system works. Crystal quality of Si(100) was of $\chi_{min} = 3.01\%$, tested by RBS/C. A Ni film thickness was measured at 240 nm. A MoC film on Si substrate with a Mo transition layer was analyzed, the film content ratio being Mo:C= 0.71:0.29, with the Mo transition layer of 296.4 nm thick. Light element analysis of TiBN film was performed by non-Rutherford elastic backscattering, the stoichiometric ratio being Ti/N/B = 1.4:1.75:1.

[1] Jeynes C, Barradas N P, Blewett M J, *et al*. Improved ion beam analysis facilities at the University of Surrey. Nucl Instrum Meth B, 1998, **136-138**: 1229–1234. DOI: 10.1016/S0168-583X(97)00818-5

[2] Lopez J G, Ager F J, Rank M B, *et al*. CNA: The first accelerator-based IBA facility in Spain. Nucl Instrum Meth B, 2000, **161-163**: 1137–1142. DOI: 10.1016/S0168-583X(99)00702-8

[3] Uhrmacher M, Hofsass H. Ion accelerator facilities at the University of Gottingen. Nucl Instrum Meth B, 2005, **240**: 48–54. DOI: 10.1016/j.nimb.2005.06.087

[4] Roumie M, Nsouli B, Zahraman K, *et al*. First accelerator based ion beam analysis facility in Lebanon: development and applications. Nucl Instrum Meth B, 2004, **219-220**: 389–393. DOI: 10.1016/j.nimb.2004.01.088

[5] Hatori S, Kurita T, Hayashi Y, *et al*. Developments and applications of accelerator system at the Wakasa Wan Energy Research Center. Nucl Instrum Meth B, 2005, **241**: 862–869. DOI: 10.1016/j.nimb.2005.07.176

[6] Pellegrino S, Trocellier P, Miro S, *et al*. The JANNUS Saclay facility: A new platform for materials irradiation,implantation and ion beam analysis. Nucl Instrum Meth B, 2012, **273**: 213–217. DOI: 10.1016/j.nimb.2011.07.078

[7] Wang Y Q and Nastasi M A. Handbook of modern ion beam materials analysis, Material Research Society, 2009.

[8] Amsel G, Battistig G. The impact on materials science of ion beam analysis with electrostatic accelerators. Nucl Instrum Meth B, 2005, **240**: 1–12. DOI: 10.1016/j.nimb.2005.06.078

[9] Chu W K, Mayer J W, Nicolet M A. Backscattering spectrometry, New York: Academic Press, 1978.

[10] He J, Lee J C, Li M, *et al*. Computerized control and operation of rutherford backscattering/channeling for an in situ ion beam system and its application for measurement of Si(001) and ZnO(001). Chin Phys Lett, 2011, **28**: 012901. DOI: 10.1088/0256-307X/28/1/012901